Archives of Biochemistry and Biophysics 505 (2011) 178–185

Contents lists available at ScienceDirect

Archives of Biochemistry and Biophysics

journal homepage: www.elsevier.com/locate/yabbi

Exploring *O*-acetylserine sulfhydrylase-B isoenzyme from *Salmonella typhimurium* by fluorescence spectroscopy

Enea Salsi [a,1], Rong Guan [c,1], Barbara Campanini [a], Stefano Bettati [a,b], Jianling Lin [d], Paul F. Cook [c,*], Andrea Mozzarelli [a,b,*]

[a] Department of Biochemistry and Molecular Biology, University of Parma, Parma, Italy
[b] Italian Institute for Biostructures and Biosystems, Rome, Italy
[c] Department of Chemistry and Biochemistry, University of Oklahoma, Norman, OK, USA
[d] Department of Biochemistry and Molecular Biology, University of Oklahoma Health Sciences Center, Oklahoma City, OK, USA

ARTICLE INFO

Article history:
Received 3 September 2010
and in revised form 4 October 2010
Available online 16 October 2010

Keywords:
Pyridoxal 5′-phosphate
Enzyme
Fluorescence
Tryptophan emission

ABSTRACT

The pyridoxal 5′-phosphate (PLP)-dependent enzyme *O*-acetylserine sulfhydrylase (OASS) catalyzes the synthesis of cysteine in bacteria and plants. In bacteria two isoenzymes are present, OASS-A and OASS-B, with distinct structural, functional, and regulatory properties. In order to gain a deeper insight into OASS-B dynamic and functional properties, single and double mutants of the three tryptophan residues, Trp28, Trp159, and Trp212, were prepared and their fluorescence emission properties were characterized in the absence and presence of substrate and ligands by steady-state and time-resolved spectrofluorimetry. Residue Trp28 was found to be mainly responsible for Trp fluorescence emission, whereas Trp212, located in a highly flexible region near the active site, is mainly responsible for an energy-transfer to PLP leading to an emission at 500 nm. Not surprisingly, mutation of Trp212 affects OASS-B activity. Trp159 slightly contributes to both direct emission and energy transfer to PLP. Time-resolved fluorescence measurements confirmed these findings, observing a third longer tryptophan lifetime for apo-OASS-B, in addition to the two lifetimes that are present in the holo-enzyme and mutants. A comparison with the emissions previously determined for OASS-A indicates that OASS-B active site is likely to be more polar and flexible, in agreement with a broader substrate specificity and higher catalytic efficiency.

Introduction

O-Acetylserine sulfhydrylase [11] (OASS)[2] is a pyridoxal 5′-phosphate (PLP)-dependent enzyme catalyzing the final step of cysteine biosynthesis in bacteria and plants, the conversion of *O*-acetyl-L-serine (OAS) and bisulfide into L-cysteine and acetate [17]. The reaction occurs via several catalytic intermediates characterized by distinct spectroscopic properties (Scheme 1) [11]. The internal aldimine (ISB, Scheme 1) is distributed between two tautomers, the ketoenamine and the enolimine. Binding of the substrate OAS forms an external Schiff base (ESB, Scheme 1), which undergoes β-elimination of acetate to give the α-aminoacrylate Schiff base (AA, Scheme 1). The nucleophilic attack of bisulphide on C-3 of AA generates L-cysteine.

In bacteria two OASS isozymes, OASS-A and OASS-B, are the products expressed by the *cysK* and *cysM* genes, respectively [16]. OASS-A is the dominant isozyme expressed under most growth conditions, while OASS-B is expressed under anaerobic growth conditions. The OASS-A and OASS-B isozymes of *Salmonella typhimurium* share 40% sequence identity, 20% high sequence similarity, and 11% sequence similarity [16]. The B-isozyme exhibits a 12-fold higher turnover number, a 10-fold decreased affinity for the substrate OAS, and a broader specificity with respect to OASS-A [11]. In addition, depending on the organism, OASS-B can use *O*-phosphoserine in place of OAS, and thiosulfate or the sulfur carrier protein CysO as alternative nucleophilic substrates [1,9,21]. The crystal structures of OASS-A and OASS-B have been determined from *S. typhimurium* [7,11], *Haemophilus influenzae* [15], *Escherichia coli* [13,27], *Arabidopsis thaliana* [6], *Entamoeba histolytica* [12], and *Mycobacterium tuberculosis* [1,2,25]. Overall, the two isozymes exhibit a very similar structural fold. However, some

* Corresponding authors. Addresses: Department of Chemistry and Biochemistry, University of Oklahoma, 620 Parrington Oval, Norman, Oklahoma 73019, USA. Fax: +1 405 325 7182 (P.F. Cook); Department of Biochemistry and Molecular Biology, University of Parma, Via GP Usberti 23/A, 43100 Parma, Italy. Fax: +39 0521 905 151 (A. Mozzarelli).
E-mail addresses: pcook@ou.edu (P.F. Cook), andrea.mozzarelli@unipr.it (A. Mozzarelli).

[1] These authors contributed equally to the work.

[2] *Abbreviations used:* OASS, *O*-acetylserine sulfydrylase; OAS, *O*-acetylserine; PLP, pyridoxal 5′-phosphate; ISB, internal Schiff base; ESB, external Schiff base; AA, α-aminoacrylate; SAT, serine acetyltransferase.

0003-9861/$ - see front matter © 2010 Elsevier Inc. All rights reserved.
doi:10.1016/j.abb.2010.10.005

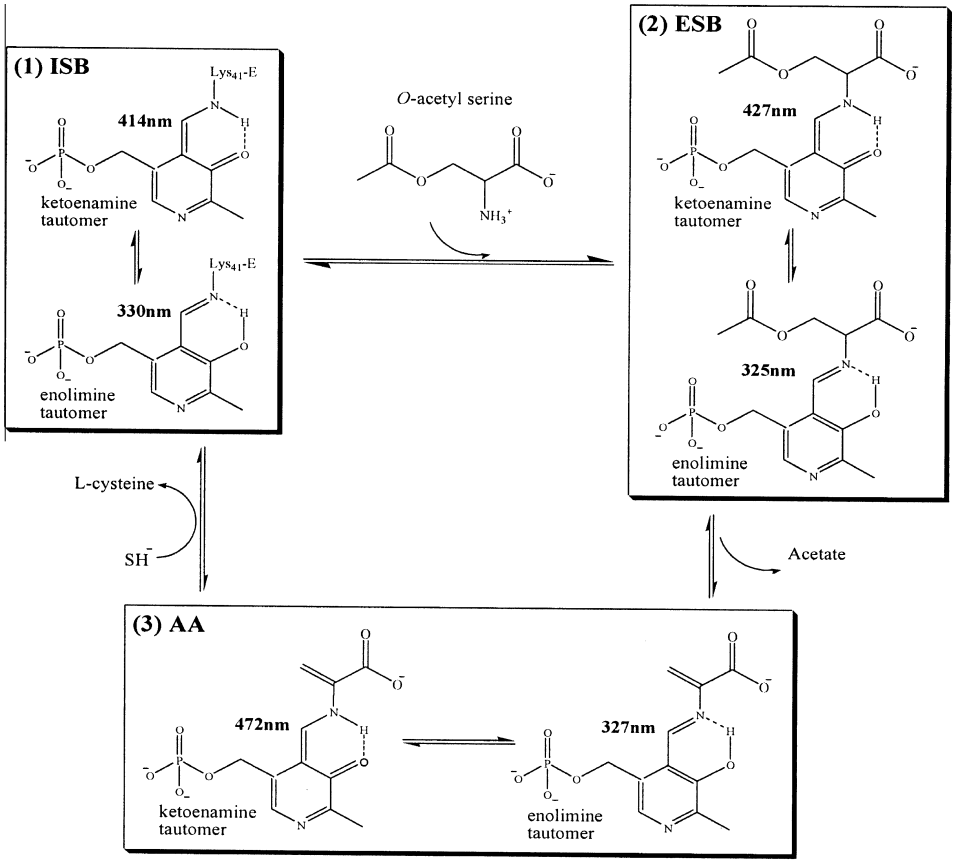

Scheme 1. Catalytic reaction of *O*-acetylserine sulfhydrylase. Absorption maxima reported below each intermediate refer to the B-isozyme.

differences are observed between OASS-B and OASS-A when comparing the crystallographic structures of the enzymes from *S. typhimurium* [11]. The average temperature factors of the crystal structure are higher for the OASS-B isoenzyme, and the active site of OASS-B is larger compared to OASS-A. The OASS-B active site is characterized by the presence of two acidic residues, Asp281 and Cys280, not present in OASS-A. Thus, the OASS-B active site is less hydrophobic compared to OASS-A, with an increased overall charge. The allosteric anion binding site, present at the dimer interface of OASS-A [8], has not been identified in the OASS-B structure. OASS-A, but not OASS-B, interacts with serine acetyltransferase (SAT), the enzyme that catalyzes the synthesis of OAS in the cysteine biosynthetic pathway, forming a bienzyme complex [17,20,22,23]. Interaction is mediated by the C-terminus of SAT, which binds to the OASS-A active site, triggering a transition from an open to a partially closed conformation [10,15,22,23]. Recent experimental and computational studies have allowed the identification of specific OASS-A pentapeptides inhibitors [23].

OASS-A and OASS-B contain two (Trp50 and Trp162) and three (Trp28, Trp159, and Trp212) tryptophan residues, respectively (Fig. 1). In OASS-B Trp159 is located in a position similar to Trp162 in OASS-A, at a distance of 21.9 Å from PLP, and Trp28 is

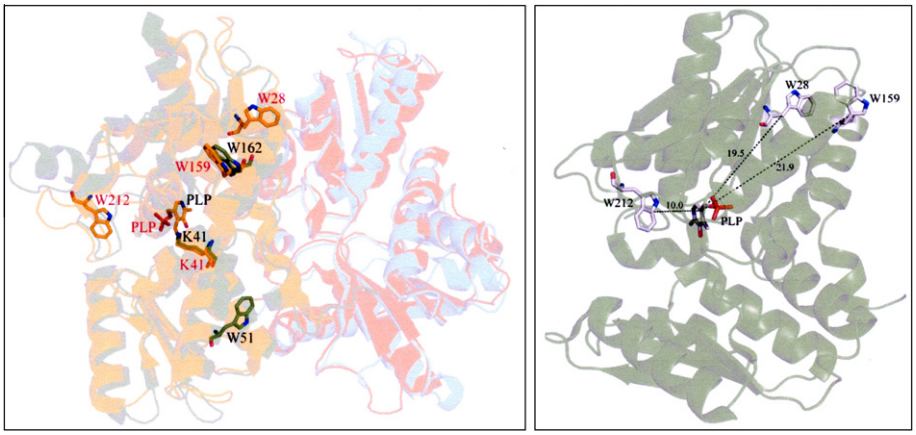

Fig. 1. A comparison between tryptophan residues in OASS-A (green) and OASS-B (yellow) is shown on the left. Relative distances between single tryptophan residues and the PLP cofactor in OASS-B are reported on the right. Figures were generated via PyMol using the following pdb files: OASS-A (1OAS) and OASS-B (2JC3). (For interpretation of the references to colour in this figure legend, the reader is referred to the web version of this article.)

in proximity to Trp159 at 19.5 Å from PLP. Trp212 has no homologue in the A isozyme and is very close to the OASS-B active site, 10.0 Å away from the PLP. Trp50 in OASS-A, the residue that is mainly involved in an energy-transfer process to the PLP cofactor [3], has no homologue in OASS-B and is substituted by a valine. In OASS-B Trp28 and Trp212 are located in highly flexible regions, characterized by elevated temperature factors in the crystal structure [11]. In particular, Trp212 is part of the loop located at the active site entrance that is responsible for the broader substrate specificity of the B isozyme with respect to the A isozyme. The presence, in this region, of bulky residues such as Arg and Trp is the hallmark of *cysM* gene products [27].

To gain insight into the dynamics of OASS-B we have characterized the steady-state and time-resolved emission properties of the isozyme from *S. typhimurium* and mutants in which tryptophan residues were individually or doubly replaced. Data were then compared to those obtained previously for OASS-A [3,19,24], providing information on the dynamics specificity of the B-isozyme.

Materials and methods

Chemicals

All chemicals and buffers were purchased from Sigma–Aldrich and were of the best available quality.

Preparation of plasmids for wild type and mutant OASS-B

The *cysM* gene encoding OASS-B from *S. typhimurium* was subcloned into a pET16b vector via the *Nde*I/*Xho*I sites, using a pRSM17 vector [11]. Site-directed mutagenesis was performed using the QuikChange® method to make three single Trp-mutant enzymes, W28Y, W159H, and W212Y, and three double Trp-mutant enzymes, W28Y/W159H, W28Y/W212F, and W159H/W212F. The template for single mutant enzymes was the plasmid encoding recombinant OASS-B, while templates for double mutant enzymes were the plasmids encoding W159H for W28Y/W159H and W159H/W212F, and W212F for W28Y/W212F. The oligonucleotide primers used to generate the mutations are listed in Table 1. The resulting mutant genes were sequenced at the Laboratory for Genomics and Bioinformatics of the University of Oklahoma Health Science Center to check for the correctness of mutations. All constructs encoded an N-terminal 10 His-tagged enzyme.

Preparation of enzymes

Wild type OASS-A from *S. typhimurium* was expressed and purified as previously reported [10]. Plasmids containing the mutated gene for OASS-B were transformed into *E. coli* BL21-(DE3)-RIL cells for expression. The strain containing the mutated plasmid was grown overnight at 37 °C in 50 mL of LB medium with 100 μg/mL ampicillin. This culture was then transferred into 1 L of LB/ampicillin medium on the morning of the next day and the cell growth was continued at 30 °C until the A_{600} reached 0.7. IPTG was then added to a final concentration of 1 mM to initiate expression. After 4 h of induction at 30 °C, the cells were harvested by centrifugation at 4500 for 30 min. The cell pellet was suspended in 50 mM phosphate, 300 mM NaCl and 10 mM imidazole, pH 8.0 and sonicated on ice for 3 min with a 30 s pulse followed by a 1 min rest, using a MISONIX Sonicator XL. The supernatant was obtained by centrifugation at 20,000*g* for 30 min and 0.05 mg/mL PLP was added, stirring at 4 °C for an hour. The supernatant was then loaded onto a Ni-NTA column with a 6 mL bed volume. The column was washed with 10 column volumes of 50 mM imidazole at pH 8.0 and the enzyme was eluted with three column volumes of 250 mM imidazole at pH 8.0. The purified enzyme was dialyzed against 5 mM Hepes, pH 8.0, and stored frozen at −80 °C. All of the mutant enzymes and the wild type enzyme were purified in the same way described above. Apo-OASS-B was prepared following a published protocol [14].

Table 1
Sequence of oligonucleotide primers.

$W28Y_f$	CGGCAGTGAAATC**TAT**GTCAAGCTGGAAGGC
$W28Y_r$	GCCTTCCAGCTTGAC**ATA**GATTTCACTGCCG
$W159H_f$	CCGGCCCGGAAATC**CAC**CGGCAAACGTCAGG
$W159H_r$	CCTGACGTTTGCCG**GTG**GATTTCCGGGCCGG
$W212F_f$	GGCATTCGACGC**TTC**CCTGCGGAATATATGCC
$W212F_r$	GGCATATATTCCGCAGG**GAA**GCGTCGAATGCC

Enzymatic assay

Initial velocity measurements of OASS activity were performed in 100 mM Hepes buffer, pH 7.0, at 25 °C using OAS and TNB as substrates. The disappearance of TNB at 412 nm (ε_{412} = 14,150 M^{-1} cm^{-1}) was monitored using a Beckman DU 640 spectrophotometer.

Rapid-scanning stopped-flow measurements

Pre-steady-state kinetic measurements monitoring OAS binding to OASS-B mutants were carried out using an OLIS-RSM 1000 stopped-flow spectrophotometer, as previously reported [11]. Separate values of k_{max} and K_{ESB} were not estimated because of difficulties in achieving saturation with OS.

Spectrophotometric measurements

UV–vis spectra of wild type OASS-B and mutant enzymes were collected at 25 °C in 100 mM Mes buffer, pH 6.5, in the absence and presence of 10 mM OAS, or in 100 mM Hepes buffer, pH 8.0, in the absence and presence of either 200 mM serine or 100 mM cysteine, using a Hewlett–Packard, model 8452A photodiode array spectrophotometer.

Steady-state fluorescence measurements

Fluorescence spectra of solutions containing 3 μM OASS-A, OASS-B, or OASS-B mutant enzymes were collected at 25 °C in 10 mM phosphate buffer, pH 6.3, in the absence and presence of 2 mM OAS, or in 100 mM Hepes buffer, pH 8.0, in the absence and presence of 250 mM serine and 5 M acetate, or in 100 mM Ches buffer, pH 9.5. Spectra of a solution containing 3 μM apo-OASS-B were collected in 100 mM Hepes buffer, pH 7.0. Emission spectra were collected upon excitation at 298 nm ($slit_{ex}$ = 3 nm, $slit_{em}$ = 5 nm), 330 nm ($slit_{ex}$ = 5 nm, $slit_{em}$ = 10 nm), 412 nm ($slit_{ex}$ = 5 nm, $slit_{em}$ = 5 nm), or 470 nm ($slit_{ex}$ = 5 nm, $slit_{em}$ = 5 nm), while excitation spectra were recorded with the emission monochromator set at 500 nm ($slit_{ex}$ = 5 nm, $slit_{em}$ = 5 nm) or 550 nm ($slit_{ex}$ = 5 nm, $slit_{em}$ = 5 nm) using a Shimadzu RF-5301 PC spectrofluorometer. All spectra were corrected for buffer contribution.

Time-resolved fluorescence measurements

Determination of fluorescence lifetime [18] of wild type OASS-B, apo-OASS-B, and mutant OASS-B enzymes was carried out at 25 °C in 10 mM phosphate buffer, pH 6.3, in the absence and presence of 2 mM OAS, using an ISS Chronos fluorescence lifetime spectrometer equipped with ISS PX01 photon counting module, ISS LA5 RF amplifier, IFR2023A 9 kHz–1.2 GHz signal generators, and LED light source. Excitation was set at 300 nm and emission was

collected for wavelengths higher than 335 nm using a cut-off filter. PPO (2,5-diphenyloxazole) and *p*-terphenyl were the lifetime standards for calibration of instrument. Data analysis was performed using the Vinci Multidimensional Fluorescence Spectroscopy Analysis software, and the minimization of χ^2 was the criterion for the selection of the best fit multi-exponential decay function.

Results

Absorbance spectroscopy

The UV–vis spectra of ISB of OASS-B exhibit a major band at 414 nm, attributed to the ketoenamine tautomer of the cofactor PLP, with a lower absorption at 330 nm attributed to the enolimine tautomer [11] (Fig. 2). In the presence of serine the band at 414 nm shifts to 427 nm with no intensity change as a result of the formation of ESB (Fig. 2). A weak intensity band at 325 nm is observed, attributed to the enolimine tautomer of PLP. In the presence of cysteine (Fig. 2) the band at 414 nm shifts to 422 nm with a decrease in the absorption intensity and a concomitant weak increase in the absorbance at 325 nm. The binding of OAS (Fig. 2) results in the disappearance of the band at 414 nm and the appearance of bands at 327 and 472 nm, attributed to the enolimine and ketoenamine tautomers of AA intermediate, respectively. The UV–vis spectra of OASS-B single and double Trp mutants all show an absorption band at 414 nm and absorbance changes in the presence of OAS and ligands as observed for the wild type enzyme (data not shown). The extinction coefficients at 414 nm were determined for wild type and mutant enzymes. The ε_{414} values (with units of $M^{-1}\,cm^{-1}$) range from 6800 to 6600 for WT, W159H/W212F, and W28Y, 6040 to 5800 for W28Y/W212F, W212F, and W159H, and about 5500 for W28Y/W159H.

Steady-state fluorescence spectroscopy

The fluorescence emission spectra of wild type OASS-B recorded for the direct excitation at 298 nm of Trp residues exhibit a pronounced peak, centered around 333 nm and a much lower intensity peak at 505 nm (Fig. 3A and B). The same two emission peaks are observed for OASS-A (Fig. 3A) [3,11]. The peak centered at 333 nm is attributed to direct emission from Trp residues, while the peak centered at 505 nm is attributed to emission from PLP, resulting from an intra-molecular energy-transfer process from the excited Trp residues to the cofactor [3]. The intensity of the direct emission is 3-fold higher for OASS-B compared to OASS-A,

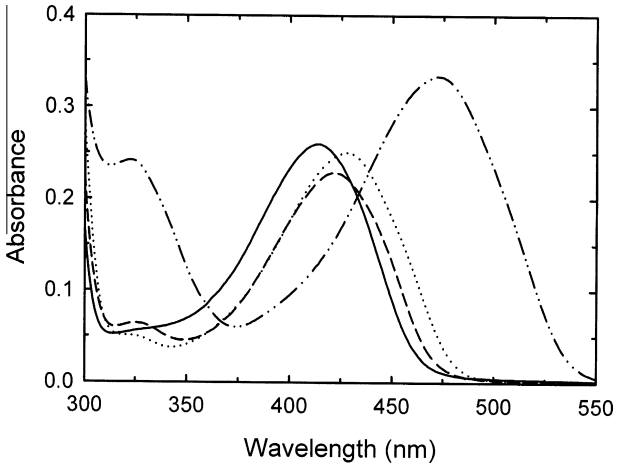

Fig. 2. Absorption spectra of wild type OASS-B in the absence (solid line) and presence of 10 mM OAS (dash-dot-dot line), 200 mM serine (dotted line) and 100 mM cysteine (dashed line).

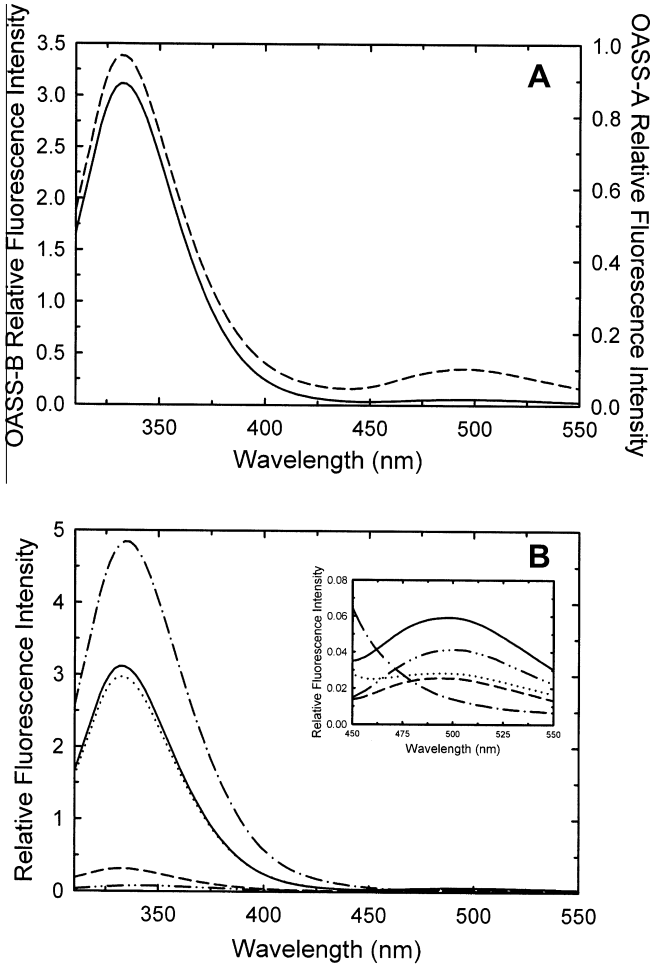

Fig. 3. (A) Fluorescence emission spectra of OASS-B (solid line) and OASS-A (dashed line) for excitation at 298 nm. The *y*-axis scale on the left and right refers to emission intensity of OASS-B and OASS-A, respectively. (B) Fluorescence emission spectra for excitation at 298 nm of holo-OASS-B (solid line), apo-OASS-B (dash-dot line), W159H/W212F holo OASS-B mutant, presenting only Trp28 (dotted line), W28Y/W212F holo-OASS-B mutant, presenting only Trp159 (dashed line) and W28Y/W159H holo-OASS-B mutant, presenting only Trp212 (dash-dot-dot line). Inset: Magnification of the region 450–550 nm.

whereas the emission intensity resulting from energy-transfer to PLP is 2-fold lower in the B isozyme. The ratio between emission intensities at 337 and 500 nm for OASS-A is 8.8, while the ratio between emission intensities at 333 and 505 nm is 52 for OASS-B. The emission spectrum obtained for apo-OASS-B (Fig. 3B) exhibits a single peak at 337 nm with a 1.6-fold increase in emission intensity compared to the holo-enzyme. In the case of apo-OASS-A the emission intensity increase was 2-fold [5]. None of the fluorescence emission properties of wild type or OASS-B mutants is affected by pH change from 6.3 to 9.5 (data not shown).

The double mutant OASS-B enzymes have only a single Trp residue, with W159H/W212F, W28Y/W212F, and W28Y/W159H having W28, W159, and W212 preserved, respectively. The emission spectra of the three double mutant enzymes, as shown in Fig. 3B, exhibit distinct fluorescence intensities. Trp28 exhibits a peak at 333 nm, that is about 95% that of wild type, and a peak at 505 nm, that is about 30% that of wild type. Similarly, Trp159 exhibits peaks at 333 and 505 nm accounting for 10% and 25%, respectively, of wild type emission. Trp212 exhibits a direct emission peak at 348 nm with a very low intensity, about 3% that of wild type, while the 505 nm emission intensity is 65% that of wild type. The emission peak centered at 348 nm suggests an exposed or partially exposed residue. The single mutant enzymes, W28Y

(containing W159 and W212), W159H (containing W28 and W212), and W212F (containing W28 and W159) exhibit spectra that are essentially the sum of the respective double mutant enzyme spectra (data not shown).

Direct excitation of the OASS-B enolimine tautomer at 330 nm gives an emission spectrum very similar to that of OASS-A, with two peaks centered at 390 and 490 nm (Fig. 4A). The peak at 390 nm is attributed to direct emission of the enolimine tautomer. However, the peak at 490 nm cannot be directly generated by excitation at 330 nm, as shown in Fig. 4C, and thus is attributed to the ketoenamine tautomer generated in the excited state [3]. The emission intensities are 3- and 1.7-fold lower in OASS-B than in OASS-A at 390 and 490 nm, respectively. Emission spectra measured for all single and double Trp mutant enzymes are similar to the wild type (Table 2). Direct excitation of the OASS-B ketoenamine tautomer of PLP at 412 nm gives a single emission peak centered at 505 nm, similar to OASS-A (Fig. 4B); the emission intensity is 2-fold lower for OASS-B compared to OASS-A. The emission spectra for the single and double Trp mutants are similar to the wild type (Table 2). The excitation spectrum of OASS-B recorded with the emission at 500 nm is also similar to that of OASS-A, exhibiting two peaks centered at 280 and 415 nm (Fig. 4C). The excitation spectra for single and double Trp mutants are similar to those of wild type.

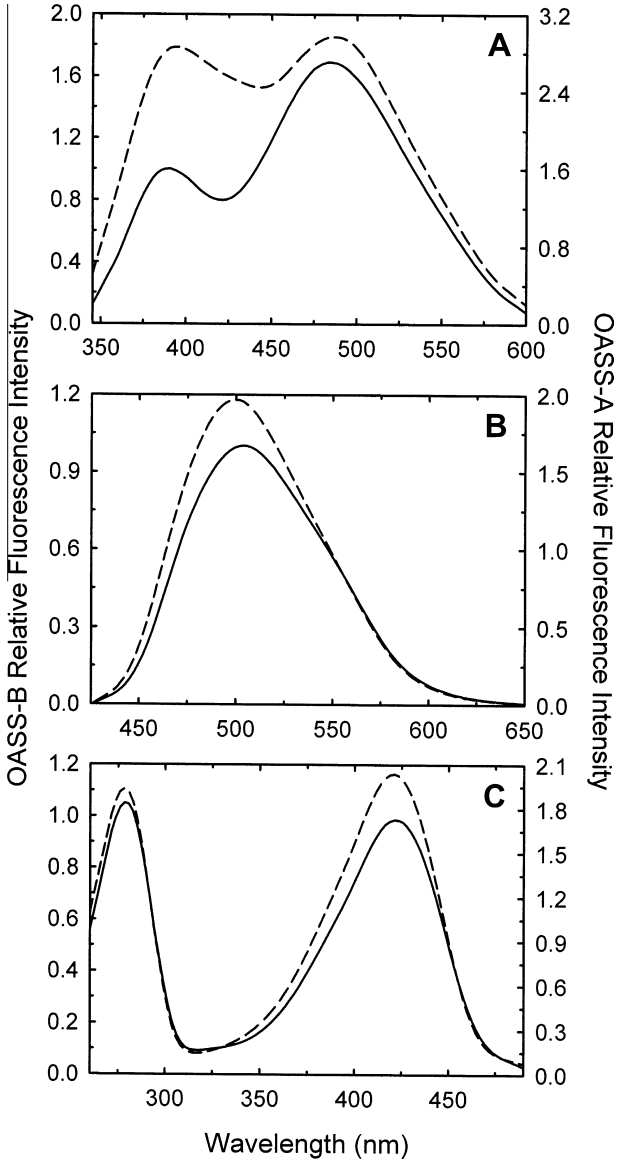

Fig. 4. Fluorescence spectra of OASS-B (solid line) and OASS-A (dashed line) for excitation at 330 nm (A), for excitation at 412 nm (B) and for emission at 500 nm (C). The *y*-axis scale on the left and right refers to emission intensity of OASS-B and OASS-A, respectively.

Table 2
Steady-state fluorescence data for wild type OASS-B and mutants.

	Relative emission intensity (ex 330 nm, em 390 nm)	Relative emission intensity (ex 330 nm, em 490 nm)
Wild type OASS-B	1.0	1.6
W28Y	1.9	1.5
W159H	1.8	1.5
W212F	1.6	1.3
W28Y/W159H	1.9	1.3
W28Y/W212F	1.9	1.6
W159H/W212F	1.7	1.4
	Relative emission intensity (ex 412 nm, em 505 nm)	Relative emission intensity in the presence of OAS (ex 470 nm, em 550 nm)
Wild type OASS-B	1.00	2.0
W28Y	0.99	1.8
W159H	0.95	1.9
W212F	0.81	2.6
W28Y/W159H	0.87	1.8
W28Y/W212F	1.00	2.4
W159H/W212F	0.82	2.3
	Relative emission at 500 nm with L-serine (ex 412 nm)	Relative emission at 500 nm with acetate (ex 412 nm)
Wild type OASS-B	9.3	9.1
W28Y	8.7	8.8
W159H	8.2	9.1
W212F	5.8	7.5
W28Y/W159H	7.2	7.5
W28Y/W212F	7.3	7.5
W159H/W212F	5.8	6.4

Fluorescence emission spectra of OASS-B were also obtained in the presence of L-serine or acetate. In the presence of either ligand, spectra are similar to those reported for OASS-A. No change in direct Trp emission, but a significant increase in the emission intensity of PLP was observed with an increase of 9-fold for OASS-B and 3.5-fold for OASS-A (data not shown). Changes are associated with occupancy of the α-carboxylate binding subsite of the active site by the ligand, followed by the closure of the active site. OASS-B single and double Trp mutants exhibit the same spectroscopic changes in the presence of serine and acetate observed for the wild type (Table 2).

In the presence of the substrate OAS, the AA is formed. The fluorescence emission spectrum of the AA of OASS-B upon excitation at 298 nm exhibits a 1.2-fold increase in the direct Trp emission at 337 nm, with a 4 nm red shift of the emission maximum with respect to the ISB. The spectrum also shows a shift in PLP emission from 505 to 550 nm (Fig. 5A). The spectrum differs from that of OASS-A in the presence of OAS, which does not exhibit any significant fluorescence emission at 505 nm, either directly from Trp, or upon energy-transfer from tryptophans [19]. Excitation of the enolimine tautomer of the AA of OASS-B at 330 nm gives no change in the intensity of direct emission, but a 4.4-fold increase in the emission of the ketoenamine with a shift in the emission maximum from 490 to 550 nm (Fig. 5B). Excitation of the AA of OASS-B at 412 nm gives an almost halved decrease in the emission intensity at 500 nm with slightly higher emission around 550 nm (Fig. 5C). Emission of the AA at 550 nm is observed upon excitation at 470 nm under the same conditions (Fig. 5C). The emission intensity of the AA at 550 nm (excitation at 470 nm) is 2-fold higher than the emission intensity of the ISB at 505 nm (excitation at 412 nm). The excitation spectrum obtained for the AA of OASS-B

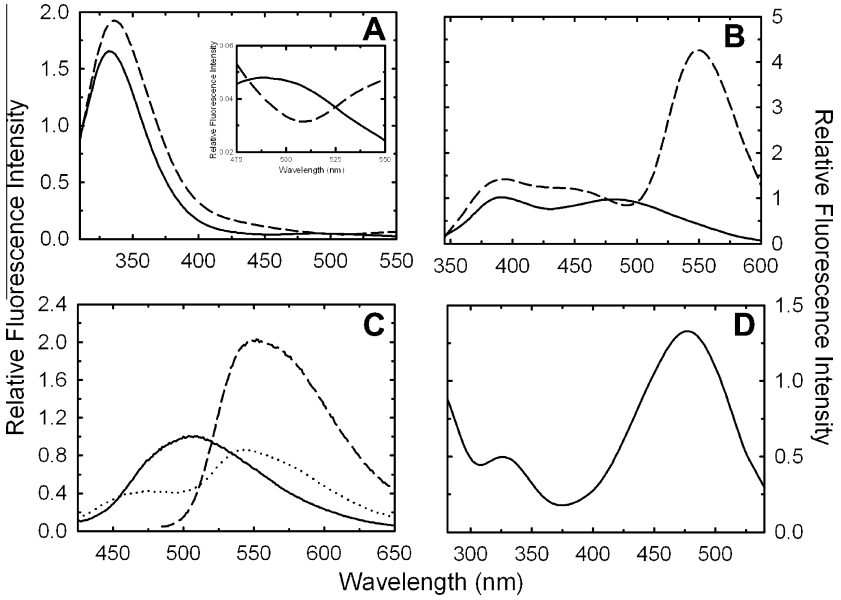

Fig. 5. Fluorescence spectra of the α-aminoacrylate intermediate of OASS-B. (A) Emission spectra for excitation at 298 nm in the absence (solid line) and presence (dashed line) of OAS. Inset: Zoom of the emission spectra in the region 475–550 nm. (B) Emission spectra for excitation at 330 nm in the absence (solid line) and presence (dashed line) of OAS. (C) Emission spectra for excitation at 412 nm in the absence (solid line) and presence (dotted line) of OAS, and for excitation at 470 nm in the presence of OAS (dashed line). (D) Excitation spectra for emission at 550 nm in the presence of OAS.

with the emission at 550 nm exhibits major bands at 280 and 470 nm with a shoulder at 330 nm (Fig. 5D). OASS-A exhibits no emission at 550 nm with excitation at 298 or 412 nm [19], or at 330 or 470 nm (data not shown). The emission spectra (excitation at 298 nm) of the AA of the double mutant enzyme W159H/W212F gave no change compared to WT (data not shown), whereas W28Y/W212F, and W28Y/W159H gave a 1.5-fold increase in Trp emission at 333 nm (Fig. 6A), and a 3.8-fold increase in Trp emission at 333 nm (Fig. 6B). Emission spectra (excitation at 298 nm) were also measured for the AA of the single mutant enzymes, W28Y, W159H, and W212F. The W28F mutant enzyme gave a 4.7-fold increase in Trp emission with a shift in the emission maximum from 333 to 348 nm compared to WT (Fig. 6C), while the W159H and W212F single mutant enzymes were similar to the WT (data not shown). All single and double Trp mutant enzymes gave spectra similar to WT upon excitation at 470 nm (Table 2).

Time-resolved fluorescence spectroscopy

Measurements of Trp fluorescence lifetime were carried out on wild type OASS-B, apo-enzyme, and single and double Trp mutants, at pH 6.3 in the absence and presence of OAS. The fluorescence lifetime values are reported in Table 3. Wild type OASS-B exhibits two lifetimes, of about 0.4 and 3 ns, which increase to 0.9 and 4 ns upon formation of the AA. The apo-enzyme shows the presence of a third longer lifetime, 8.4 ns, attributed to Trp residues quenched by PLP in the holo-enzyme. The W159H/W212F mutant enzyme (containing Trp28) exhibits two lifetimes very similar to those observed for WT affected very slightly by the formation of AA. The W28Y/W212F mutant enzyme (containing Trp159) exhibits lifetimes that do not change as the AA is formed. The W28Y/W159H mutant enzyme (containing Trp212) also exhibits two lifetimes that, however, increase significantly as the AA is formed, especially the longer one (τ = 7.6 ns), which approaches the longer lifetime detected for the apo-enzyme (τ = 8.4 ns). The same behavior was observed for the W28Y single mutant (data not shown). The W159H and W212F single mutants exhibit lifetimes very similar to those of WT (data not shown).

Kinetic characterization of OASS-B mutants

To evaluate the influence of mutations on OASS-B catalytic function, initial velocity measurements with OAS and TNB were carried out. The resulting rate constants are summarized in Table 4. The first half of the OASS-B catalyzed ping pong reaction shows an 8- to 10-fold decrease in the second order rate constant, $V/K_{OAS}E_t$, for all mutant enzymes in which Trp 212 is mutated, when compared to WT. Otherwise, all mutant enzymes exhibit similar kinetics to WT. In addition, rapid scanning stopped-flow measurements were carried out to measure the rate of formation of the AA in the reaction between OASS-B mutant enzymes and OAS. At most, a 5-fold decrease is observed in k_{max}/K_{OAS}, with the largest changes observed for the W212 mutations.

Discussion

In the present work, absorption and fluorescence spectroscopic properties of OASS-B from *S. typhimurium* were characterized and compared to those of the OASS-A isozyme. In addition, single and double tryptophan mutants of OASS-B were prepared and characterized in order to gain information about the role of these residues in the enzymatic reaction, and were used to compare the dynamic properties of different regions of the two isoenzymes. Results indicate that the absorption properties of the OASS-B isozyme are very similar to those observed for the A isozyme. UV–vis absorbance spectra indicate that the PLP cofactor in OASS-B is mostly present as the ketoenamine form, as in OASS-A, although a higher amount of the enolimine tautomer is present. The enolimine tautomer concentration increases when the ESB with serine or lanthionine is formed,[3] as well as when the AA is formed in the reaction with OAS.

Steady-state fluorescence measurements indicate that Trp emission resulting from direct Trp excitation is higher in OASS-B compared to OASS-A, as expected due to the presence of three Trp residues in the B isozyme and two in the A isozyme, respec-

[3] Addition of cysteine to OASS results in a rapid transient formation of the AA followed by attack by a second cysteine thiol to generate the lanthionine ESB [26].

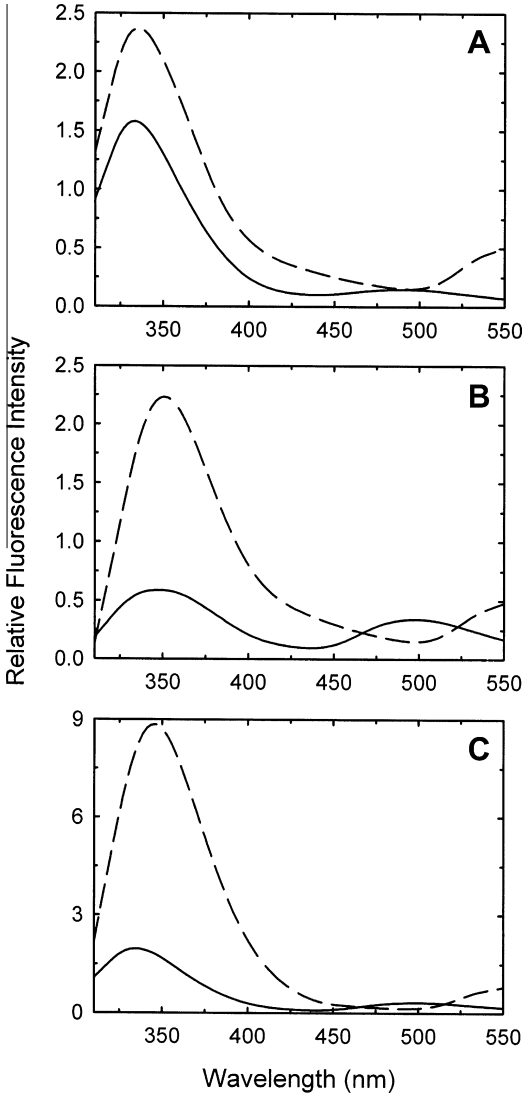

Fig. 6. Fluorescence emission spectra for excitation at 298 of the α-aminoacrylate intermediate for OASS-B mutants. (A) W28Y/W212F mutant, presenting only Trp159 in the absence (solid line) and presence (dashed line) of OAS. (B) W28Y/W159H mutant, presenting only Trp212 in the absence (solid line) and presence (dashed line) of OAS. (C) W28Y mutant presenting both Trp159 and Trp212 in the absence (solid line) and presence (dashed line) of OAS.

Table 3
Fluorescence lifetimes of Trp in the absence and presence of OAS.

	χ^2	f_1 (%)	τ_1 (ns)	f_2 (%)	τ_2 (ns)	τ_3 (ns)
apo-OASS-B[a]	0.99	0.32	0.43	0.22	2.96	8.41

	χ^2	f_1 (%)	τ_1 (ns)	τ_2 (ns)
wt OASS-B	1.80	0.20	0.44	3.37
+OAS	2.90	0.60	0.91	4.03
Trp28	1.09	0.20	0.34	3.46
+OAS	2.91	0.43	0.63	3.46
Trp159	2.74	0.61	0.55	2.23
+OAS	3.16	0.93	0.82	2.93
Trp212	1.81	0.60	0.42	2.96
+OAS	3.06	0.68	0.74	7.57

[a] These values were determined at pH 8.0, and all others were determined at pH 6.3. χ^2 is the parameter for the evaluation of the goodness of the fit to a multi-exponential decay function. f_i represents the fractional intensity of the calculated lifetimes τ_i. The sum of f_i is 1.

Table 4
Kinetic parameters for wild type OASS-B and Trp mutants.

Enzyme	Steady-state $V/K_{OAS}E_t$ (M^{-1} s^{-1})	Pre-steady-state k_{max}/K_{OAS} (M^{-1} s^{-1})
WT	$(3.5 \pm 1.3) \times 10^4$	$(4.45 \pm 0.20) \times 10^3$
W28Y	$(8.1 \pm 0.4) \times 10^4$	$(1.67 \pm 0.02) \times 10^4$
W159H	$(5.1 \pm 0.2) \times 10^4$	$(1.02 \pm 0.01) \times 10^4$
W212F	$(3.1 \pm 0.1) \times 10^3$	$(1.70 \pm 0.20) \times 10^3$
W28Y/W159H	$(8.0 \pm 1.0) \times 10^4$	$(1.59 \pm 0.04) \times 10^4$
W28Y/W212F	$(4.6 \pm 0.1) \times 10^3$	$(1.20 \pm 0.20) \times 10^3$
W159H/W212F	$(3.1 \pm 0.1) \times 10^3$	$(0.82 \pm 0.08) \times 10^3$

tively. However, the quantum yield of PLP fluorescence emission is 2-fold lower in OASS-B, possibly due to the larger and more polar active site of the B isozyme. A lower efficiency in the energy transfer process from the Trp(s) to the cofactor is also observed in OASS-B. In fact, the Trp residue that mainly accounts for the energy transfer in the A isozyme, i.e., Trp50 [3], is absent in the structure of OASS-B (Fig. 1). Thus, the ratio between direct Trp emission and PLP emission resulting from energy-transfer is 6-fold higher for OASS-B compared to OASS-A. In the presence of serine and acetate similar molecular events occur at the OASS-B active site as for OASS-A, suggesting that the occupation of the α-carboxylic subsite triggers the transition from the open to the closed conformation of the enzyme. A striking difference between the two isozymes is observed in the steady-state fluorescence spectra. Formation of the AA exerts different effects on the emission properties of the two isoenzymes. In OASS-A, the AA (absorbing at 325 and 470 nm) does not exhibit any significant fluorescence emission, either as a result of direct excitation or upon energy-transfer from Trp residues [19], while both the enolimine and the ketoenamine tautomers of the OASS-B AA show significant fluorescence emission. In particular, the quantum yield for direct fluorescence emission from the AA ketoenamine tautomer is 2-fold higher than that of the ketoenamine tautomer of the ISB, probably due to the closure of the active site, and in addition, the AA is still involved in energy-transfer from the excited Trp residues. These findings suggest that the active site microenvironment in the presence of the AA differs for the A and B isoenzymes, and that PLP and Trp residues in OASS-B retain a reciprocal orientation when the AA is formed that is similar to that present in the ISB, perhaps a result of tighter binding of the cofactor.

Mutation of Trp does not affect PLP spectrophotometric properties of OASS-B, but alters enzymatic activity for some of the mutant enzymes. The effect of mutating Trp28 and Trp159 is minimal, with 2.5-fold and a 1.5-fold decreases observed, respectively, on the second order rate constant for the first half reaction measured in the steady state and pre-steady state, Table 4. However, mutation of Trp212, a residue very close to the active site, causes an 11-fold decrease in the rate constant. Trp212 is included in a loop that is considered as one of the hallmarks for classification of an *O*-acetylserine sulfhydrylase as an A or B isozyme (9). In the A isozyme the loop is shorter and contains small residues such as Gly and Ala, whereas in the B isozyme it is larger and contains residues such as Arg, Trp, and Met. It is perhaps not surprising that activity is lost as this residue is mutated.

Direct Trp fluorescence emission is 1.6-fold higher for apo-OASS-B than for the wild type enzyme indicating that emission from Trp residues is quenched by PLP due to energy transfer. Time-resolved fluorescence measurements confirmed this finding since a longer tryptophan lifetime is observed for apo-OASS-B, in addition to the two lifetimes that are also present in the holo-isozyme B and A [4]. A small increase in direct Trp emission is also observed for wild type OASS-B in the presence of OAS, suggesting that part of the quenching effect is relieved when the AA is formed.

Trp28 alone accounts for almost all of the direct Trp emission in OASS-B, but is minimally involved in energy-transfer to PLP. Trp28 is far from the PLP and is located in the vicinity of Trp159, a homologue of Trp162 in OASS-A that accounts for most of the direct Trp emission in the A isoenzyme. The emission maximum of Trp28 is centered at 333 nm, slightly blue-shifted compared to the 337 nm Trp emission maximum in OASS-A, indicating that its microenvironment is less solvent exposed compared to Trp162 in OASS-A. Residue Trp212 is the closest to the active site and is almost completely solvent exposed, as pointed out by its direct emission peak centered at 348 nm; emission from this residue is strongly quenched by PLP. In fact, Trp212 alone accounts for only 3% of the direct Trp emission, but 65% of the total Trp energy-transfer to the cofactor. The 4 nm red shift in the Trp emission maximum observed for apo-OASS-B can be attributed to an increase in direct emission from Trp212 in the apo-enzyme. In the presence of OAS, Trp212 exhibits a strong increase in direct emission for excitation at 298 nm, and an increase in its longer lifetime that becomes similar to the value observed for apo-OASS-B. Thus, Trp212 is mainly responsible for the increase in direct tryptophan emission observed for wild type OASS-B in the presence of OAS, associated with a 4 nm red shift. Trp159 exhibits very low direct emission and has a minor role in energy-transfer to the PLP.

Time-resolved fluorescence measurements indicate that wild type and double Trp mutants' emission decays are accounted for by two lifetimes, about 0.4 and 3 ns, almost independent of the emitting Trp residue. Trp159 and Trp212 emissions are more significantly accounted for by the short lifetime ($f_1 = 0.60$) (Table 3) whereas Trp28 emission exhibits essentially the same f_1 as the wild type (0.2) (Table 3). These findings are in agreement with the lower intensity of Trp159 and Trp212 steady-state fluorescence with respect to wild type and Trp28 (Fig. 3). Similar lifetimes were measured for OASS-A, $\tau_1 = 0.48$ ns, and $\tau_2 = 2.28$ ns with $f_2 = 0.70$ [3].

The longer lifetime (8.4 ns) that accounts for about 46% of the emission decay in the apo-OASS-B is likely associated with Trp residues that contribute to the energy transfer process and emission at 505 nm, i.e., predominantly Trp212, and to a lesser extent Trp28 and Trp159. It is interesting to note that (i) Trp212 has no homologue in OASS-A and (ii) apo-OASS-A does not show a long lifetime. In OASS-A, the apo-fluorescence intensity increase is mainly accounted for by both a longer τ_2 and a higher τ_2 fraction ($\tau_2 = 4.1$ ns and $f_2 = 0.91$). A long lifetime also accounts for the emission decay of Trp212 of OASS-B in the presence of OAS ($\tau_1 = 0.74$ ns and $\tau_2 = 7.57$ ns with $f_2 = 0.32$) (Table 3). A long lifetime, $\tau_3 = 6.9$, $f_3 = 0.62$, was also observed for OASS-A in the presence of OAS, although the overall steady-state emission intensity was lower than that observed for OASS-B in the presence of OAS. Thus, the red emission band at about 550 nm of AA intermediate is associated with long lifetimes. These data indicate that the formation of the catalytic intermediate has altered the cofactor environment leading to the stabilization of the AA ketoenamine excited state. Since the emission intensity is the result of overlapping decay processes, controlled by many parameters, including polarity and flexibility, in OASS-A the resulting AA emission intensity is very low whereas it is higher in OASS-B, in spite of common emission lifetimes.

Conclusions

The spectroscopic investigation of several OASS-B catalytic intermediates shows the relevance of this approach for the detection of structural and dynamic differences between similar proteins. Overall, OASS-A and OASS-B exhibit very similar absorbance and fluorescence properties, taking into account the different number and location of Trp residues. However, at the stage of the AA, major differences were clearly detected, possibly associated with distinct dynamic properties of the protein matrix and changes in active site polarity. Moreover, via the use of single and double Trp mutants of OASS-B it was possible to assign specific contributions to each Trp residue. In particular, Trp28 is mainly responsible for fluorescence emission upon direct Trp excitation. Energy-transfer to the PLP cofactor results in significant quenching of Trp212, which is located in a highly flexible region close to the active site.

Acknowledgments

This work was carried out with the support of the International Collaborative project of Italian Ministry of University and Research and COFIN 2007 to A.M. and PFC and from the Grayce B. Kerr endowment to the University of Oklahoma to support the research of PFC.

References

[1] D. Agren, R. Schnell, W. Oehlmann, M. Singh, G. Schneider, J. Biol. Chem. 283 (2008) 31567–31574.
[2] D. Agren, R. Schnell, G. Schneider, FEBS Lett. 583 (2009) 330–336.
[3] S. Benci, S. Bettati, S. Vaccari, G. Schianchi, A. Mozzarelli, P.F. Cook, J. Photochem. Photobiol. B 48 (1999) 17–26.
[4] S. Benci, S. Vaccari, A. Mozzarelli, P.F. Cook, Biochim. Biophys. Acta 1429 (1999) 317–330.
[5] S. Bettati, S. Benci, B. Campanini, S. Raboni, G. Chirico, S. Beretta, K.D. Schnackerz, T.L. Hazlett, E. Gratton, A. Mozzarelli, J. Biol. Chem. 275 (2000) 40244–40251.
[6] E.R. Bonner, R.E. Cahoon, S.M. Knapke, J.M. Jez, J. Biol. Chem. 280 (2005) 38803–38813.
[7] P. Burkhard, G.S. Rao, E. Hohenester, K.D. Schnackerz, P.F. Cook, J.N. Jansonius, J. Mol. Biol. 283 (1998) 121–133.
[8] P. Burkhard, C.H. Tai, J.N. Jansonius, P.F. Cook, J. Mol. Biol. 303 (2000) 279–286.
[9] K.E. Burns, S. Baumgart, P.C. Dorrestein, H. Zhai, F.W. McLafferty, T.P. Begley, J. Am. Chem. Soc. 127 (2005) 11602–11603.
[10] B. Campanini, F. Speroni, E. Salsi, P.F. Cook, S.L. Roderick, B. Huang, S. Bettati, A. Mozzarelli, Protein Sci. 14 (2005) 2115–2124.
[11] A. Chattopadhyay, M. Meier, S. Ivaninskii, P. Burkhard, F. Speroni, B. Campanini, S. Bettati, A. Mozzarelli, W.M. Rabeh, L. Li, P.F. Cook, Biochemistry 46 (2007) 8315–8330.
[12] K. Chinthalapudi, M. Kumar, S. Kumar, S. Jain, N. Alam, S. Gourinath, Proteins 72 (2008) 1222–1232.
[13] M.T. Claus, G.E. Zocher, T.H. Maier, G.E. Schulz, Biochemistry 44 (2005) 8620–8626.
[14] R. Guan, S.A. Nimmo, K.D. Schnackerz, P.F. Cook, Arch. Biochem. Biophys. 487 (2009) 85–90.
[15] B. Huang, M.W. Vetting, S.L. Roderick, J. Bacteriol. 187 (2005) 3201–3205.
[16] N.M. Kredich, J. Biol. Chem. 246 (1971) 3474–3484.
[17] N.M. Kredich, M.A. Becker, G.M. Tomkins, J. Biol. Chem. 244 (1969) 2428–2439.
[18] J.R. Lakowicz, Principles of Fluorescence Spectroscopy, Plenum Press, New York, 1983.
[19] G.D. McClure Jr., P.F. Cook, Biochemistry 33 (1994) 1674–1683.
[20] K. Mino, T. Yamanoue, T. Sakiyama, N. Eisaki, A. Matsuyama, K. Nakanishi, Biosci. Biotechnol. Biochem. 64 (2000) 1628–1640.
[21] S.E. O'Leary, C.T. Jurgenson, S.E. Ealick, T.P. Begley, Biochemistry 47 (2008) 11606–11615.
[22] E. Salsi, B. Campanini, S. Bettati, S. Raboni, S.L. Roderick, P.F. Cook, A. Mozzarelli, J. Biol. Chem. 285 (2010) 12813–12822.
[23] E. Salsi, A. Bayden, F. Spyrakis, A. Amadasi, B. Campanini, S. Bettati, P. Cozzini, G.E. Kellogg, P.F. Cook, T. Dodatko, S.L. Roderick, A. Mozzarelli, J. Med. Chem. 53 (2010) 345–356.
[24] K.D. Schnackerz, C.H. Tai, J.W. Simmons 3rd, T.M. Jacobson, G.S. Rao, P.F. Cook, Biochemistry 34 (1995) 12152–12160.
[25] R. Schnell, W. Oehlmann, M. Singh, G. Schneider, J. Biol. Chem. 282 (2007) 23473–23481.
[26] E.U. Woehl, C.H. Tai, M.F. Dunn, P.F. Cook, Biochemistry 35 (1996) 4776–4783.
[27] G. Zocher, U. Wiesand, G.E. Schulz, FEBS J. 274 (2007) 5382–5389.